Study of UV and IR laser radiation interaction with metals and dielectrics

A.V. Fedenev, E.I. Lipatov, A.N. Panchenko, V.M. Orlovskii, V.F. Tarasenko, N.N. Koval, and I.M. Goncharenko

Institute of High-Current Electronics, Siberian Branch of the Russian Academy of Sciences, Tomsk

Received November 23, 2001

A complex of laser setups was created for investigation of the laser radiation interaction with metal and dielectric surfaces based on the accelerators and high-power pulsed voltage generators developed at the Institute of High-Current Electronics. The complex consists of laser systems operating in the UV and IR ranges (pulse duration is 10 ns to 100 μs, pulse power is up to 2 kJ, average laser radiation power is up to 1 kW), a chamber for samples location (pressure range is from 10^{-5} Torr to 10 atm), as well as spectroscopic and measuring equipment. The paper presents the experimental results on investigation of the laser plasma formation and propagation in vacuum and gases, laser breakdown in the high pressure SF_6 gas, as well as irradiation of a diamond by UV laser radiation and interaction of IR laser radiation with a steel surface.

A number of high pressure gas mixture lasers have been created on a basis of the electron beam accelerators and high power pulsed voltage generators developed at the Institute of High-Current Electronics SB RAS.[1–9] To study the laser radiation effect on some substance, we selected the XeCl*, CO_2, and HF lasers, as well as atomic xenon laser in the view of their high power, energy, and high efficiency.

The goal of this paper is to show the laser setups for studying the interaction of laser radiation with metals and dielectrics and to give the preliminary results of the experiments.

1. Experimental equipment

As excitation sources we used the accelerators with radial-convergent and planar electron beams, as well as setups with a self-maintained discharge and a discharge initiated by an electron beam. The main characteristics of the experimental laser setups are given in Table 1.

Table 1. Specifications of laser setups

Setups	Pumping, active volume, frequency of pulse repetition	Transitions, wavelengths, gas mixture, pressure	Pulse length, energy, efficiency	Notes
DM	Electronic beam, j = 40 A/cm^2, 600 l, aperture D = 60 cm, monopulse	XeCl, 308 nm, Ar–Xe–HCl, p = 2 atm	300 ns, 2000 J, 4%	Refs. 2, 8
		Xe, 1.73; 2.03 μm, Ar–Xe, He–Ar–Xe p = 1.0–2 atm	300 ns, 100; 50 J, ~ 1%	Refs. 2, 4
Coaxial	Electronic beam, I = 5–500 A, 200 kW, 20 l, aperture D = 20 cm, 0.1–50 Hz	Xe, 1.73; 2.03 μm, Ar–Xe, He–Ar–Xe, p = 1.0–1.5 atm	10–1000 μs, 6 J, 2%	Water cooling of foil Ref. 1
ELON-1M	Electronic beam, j = 40 A/cm^2, 30 l, aperture D = 20 cm, monopulse	XeCl, 308 nm, Ar–Xe–HCl, p = 2.5 atm	300 ns, 110 J, 5%	Ref. 3
		Xe, 1.73; 2.03 μm, Ar–Xe, He–Ar–Xe	700 ns, 16 J, ~ 2%	
		HF (nonchain) ~ 2.6–3 μm, SF_6–H_2	700 ns, 200 J, 10%	Refs. 6, 7
Cascade	Discharge initiated by an electron beam, 72×3×2.4 cm, 0.1–50 Hz	CO_2, 10.6 μm, N_2–CO_2–H_2	15 ns – 8 μs, 30 J, 1 kW (50 Hz)	System of gas cooling and circulation, Ref. 8
LIDA-T	Self-maintained discharge, 3.5×1.5×60 cm, 1–5 Hz	XeCl, 308 nm, Ne–Xe–HCl, p = 2–3 atm	100–450 ns, 0.2–1.0 J, 1–2%	Generator with inductive power accumulator, Ref. 5
		HF (nonchain) ~ 2.6–3 μm, SF_6–H_2	350 ns, 2 J, 2.9%	Ref. 9

0235-6880/02/03 258-05 $02.00

The maximum laser radiation output power up to 2 kJ in the UV spectral range was obtained at λ = 308 nm for XeCl laser with electron beam pumping of active volume of 600 l.[2,8] At the same experimental setup the output power of laser generation of 100 and 50 J was attained[4] using the Ar–Xe (λ = 1.73 μm) and He–Ar–Xe (λ = 2.03 μm) mixtures. The laser output powers of 110 J at λ = 308 nm and 90 J at λ = 249 nm were demonstrated at the setup pumped by a high-power radial-convergent beam of 30 l gas volume with 20 cm output aperture of laser radiation.[3,8] A choice of pumping geometry with a radial-convergent electron beam was found to be successful for exciting a nonchain HF laser. The output generation power up to 200 J with the efficiency to 10%, relative to the beam power put in the gas, was derived at the HF molecule transition at λ ~ 2.8 μm.[6,7]

The mean output power of laser radiation up to 1 kW was realized based on the CO_2 laser excited by a discharge with preionization by an electron beam at the pulse repetition rate of 50 Hz.[8] The use of the inductive power accelerator for pumping the nonchain electrical discharge HF laser made it possible to obtain the laser generation with the efficiency to 5.5% relative to the power put in gas. Application of the zeolite absorber increased the time of operation up to 1000 pulses[9] without changing the gas mixture. To produce a prepulse in a gas-discharge XeCl laser, we used a generator with an inductive accumulator. This enabled us to form a highly homogeneous discharge and to increase the pulse duration to 450 ns at the output generation power to 1.1 J and the total generation efficiency of 2.2% (Refs. 5, 8).

2. Experimental Results and Discussion

Absorption of UV radiation in diamond

Owing to such unique characteristics of diamond as short lifetime of charge carriers, high heat conductivity, and radiation stability, it is a very promising material. The sensitivity of diamond to UV radiation determines a possibility of its use as a laser radiation receiver or a commutator with UV-radiation control. In the experiments we used a 3×1×0.5 mm crystal of IIa-type mounted in a SMA joint. To measure the sensitivity parameters, time response, and radiation stability, the diamond detector was irradiated by the excimer laser radiation. The laser radiation ranged from 220 to 355 nm; in that case the specific power of the radiation was 100 MW/cm^2. The results of the experiment (Fig. 1) indicate that the diamond sensitivity depends on the wavelength and can vary from 10^{-4} to 10^{-2} A/W at variations of the diamond geometry and the experimental conditions. The threshold density of the diamond destruction is more than 100 MW/cm^2 and the time resolution is better than 1 ns. These physical properties make the diamond a promising instrument for measuring the radiation parameters of high-power pulse lasers.[10]

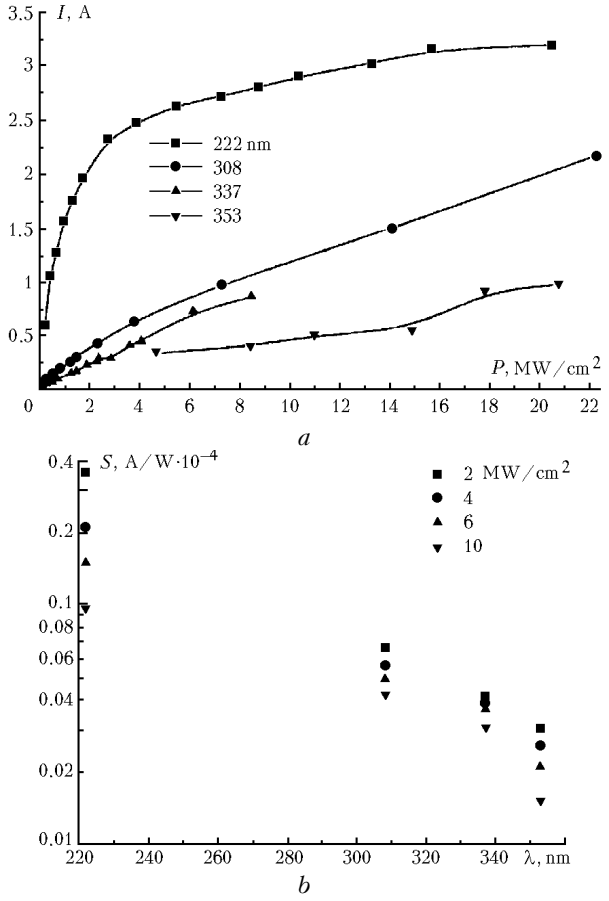

Fig. 1. The current pulse amplitude through a diamond depending on the wavelength and the laser radiation specific power (*a*). The response of a diamond detector measured for different wavelengths vs. the radiation specific power (*b*).

Expansion of laser plasma in gas and vacuum

The process of plasma formation on the surface of metals and dielectrics under irradiation by the XeCl and KrCl lasers was studied. Thresholds of plasma formation and rates of plasma expansion were measured. We have discovered that the long-lived plasma objects are formed close to the target surface in the presence of xenon or air at a pressure of 0.1–1 atm. The duration of glow of plasma objects was maximal in xenon. It was shown that laser plasma is formed during several nanoseconds after the beginning of a laser pulse. The rates of plasma expansion were several tens of km per second. When focusing a laser beam to a small conical hole (2 mm in diameter and 3 mm in length) on a metal surface, plasma jets can be formed with definite boundaries and the expansion rate of the order of 50 km/s (Fig. 2).

The effects of asymmetric current passage through laser plasma and its break were demonstrated. The current break time was about 10 ns; in that case the increase rate of the plasma electric resistance was 10^{10} Ω/s. The rate of the current break increases, when using elements with small atomic weight for creating plasma, as well as at large rates of the current rise before the break. The

degree of plasma ionization was saturated before the current break. The effect of current break was used for creation of a generator with an inductive energy accumulator. The generator with a plasma erosion current chopper, inductive energy accumulator, and chopping current of 10 kA could operate at the pulse repetition frequency up to several Hz and was successfully used for pumping the pulse lasers.

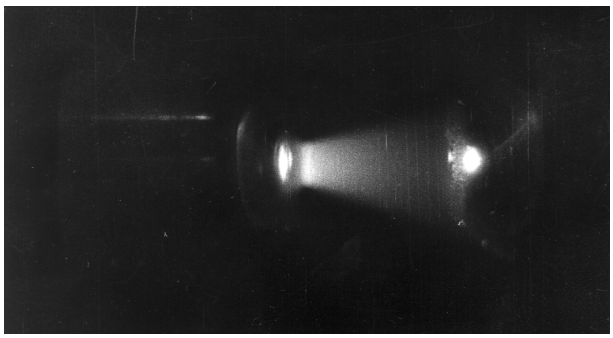

Fig. 2. Plasma jet in vacuum. The radiation of XeCl laser is focused on a conical hole (2 mm in diameter, 3 mm in depth) on the aluminum surface (laser radiation is at the left of the photograph).

Laser initiation of a megavolt gas-discharge arrester

Table 2 shows the results of the use of exciplex lasers for initiation of megavolt gas-discharge arresters.[11] Minimal delay time between the laser pulse and the start of the gas-discharge arrester was about 10 ns with the spread of 1 ns. We obtained data characterizing plasma broadening in the gap between electrodes of the arrester, as well as plasma generation on the surface of a metal target exposed to UV radiation. Owing to the minimal thresholds of plasma generation on its surface, tantalum can be recommended as a promising material for producing the arrester electrode initiated by UV laser radiation. It is shown that the delay time of the arrester start and the spread of the delay time are minimal when using laser radiation with small divergence and optical breakdown in a working gas.

Interaction of laser radiation with metal surface

In the experiments, an electric discharge nonchain HF laser with the pulse power of 2 J and pulse duration of 350 ns was used. The samples under study (carbon steel 4140 and stainless steel SUS304) were irradiated in the open air or in vacuum. The variation of surface strength in the laser print area and the variation of metal structure depending on the laser radiation power density have been examined. It was shown that as a result of displacement of liquid metal from the epicenter of interaction of radiation with the surface, microcraters of ~1 μm depth were formed. The melt layers, cooling on the adjacent surface, formed the multilayer influxes over an area of 3–4 mm^2 in the form of concentric belts. We recognized 5 characteristic zones of metal cooling. We observed the increase of the material removal with the advance of a beam focus deep into the sample. In that case the quantity of the material removed from the surface per one pulse was about $4 \cdot 10^{-4}$ g/cm^2.

Table 2. Delay and spread of operation of megavolt arrester started by UV laser radiation focused on the electrode surface (λ = 350 nm)

U_S, MV	U_S/U_{SBR}, %	P, bar	Gas mixture	Q_{LAS}, mJ	t_{DEL}, ns	σ, ns
1.02	89	2.5	SF_6	45	66	5
1.02	89	2.5	SF_6	30	183	30
1.02	89	2.5	SF_6	30	73	7
0.99	91	5	10%SF_6 + 90%N_2	45	56	10
0.99	91	5	10%SF_6 + 90%N_2	30	93	20
1.02	91	10	30%SF_6 + 70%Ne	45	73	34
0.86	90	6	8%SF_6 + 92%Ar	45	16	2
0.93	90	7	9%SF_6 + 91%Kr	52	15	1
0.99	91	4	30%SF_6 + 70%Kr	50	18	2
0.93	93	3.2	53%SF_6 + 47%Kr	50	36	14
0.99	94	2.7	70%SF_6 + 30%Kr	50	51	16
0.95	91	5	9%SF_6 + 17%N_2 + 74%Kr	52	17	1
0.93	94	5	10%SF_6 + 45%N_2 + 45%Kr	52	17	2.3
0.99	91	5.1	10%SF_6 + 60%N_2 + 30%Kr	50	13	1.3
0.99	91	4.5	10%SF_6 + 75%N_2 + 15%Kr	50	25	7
0.93	91	7	10%SF_6 + 90%Xe	50	15	2
0.93	91	6	10%SF_6 + 15%N_2 + 75%Xe	50	15	1.5
0.91	92	5	10%SF_6 + 45%N_2 + 45%Xe	50	18	2

Note: U_S is the arrester voltage, U_{SBR} is the voltage of arrester self-breakdown, Q_{LAS} and λ are power and wavelength of laser radiation, t_{DEL} and σ are delay and spread of arrester operation.

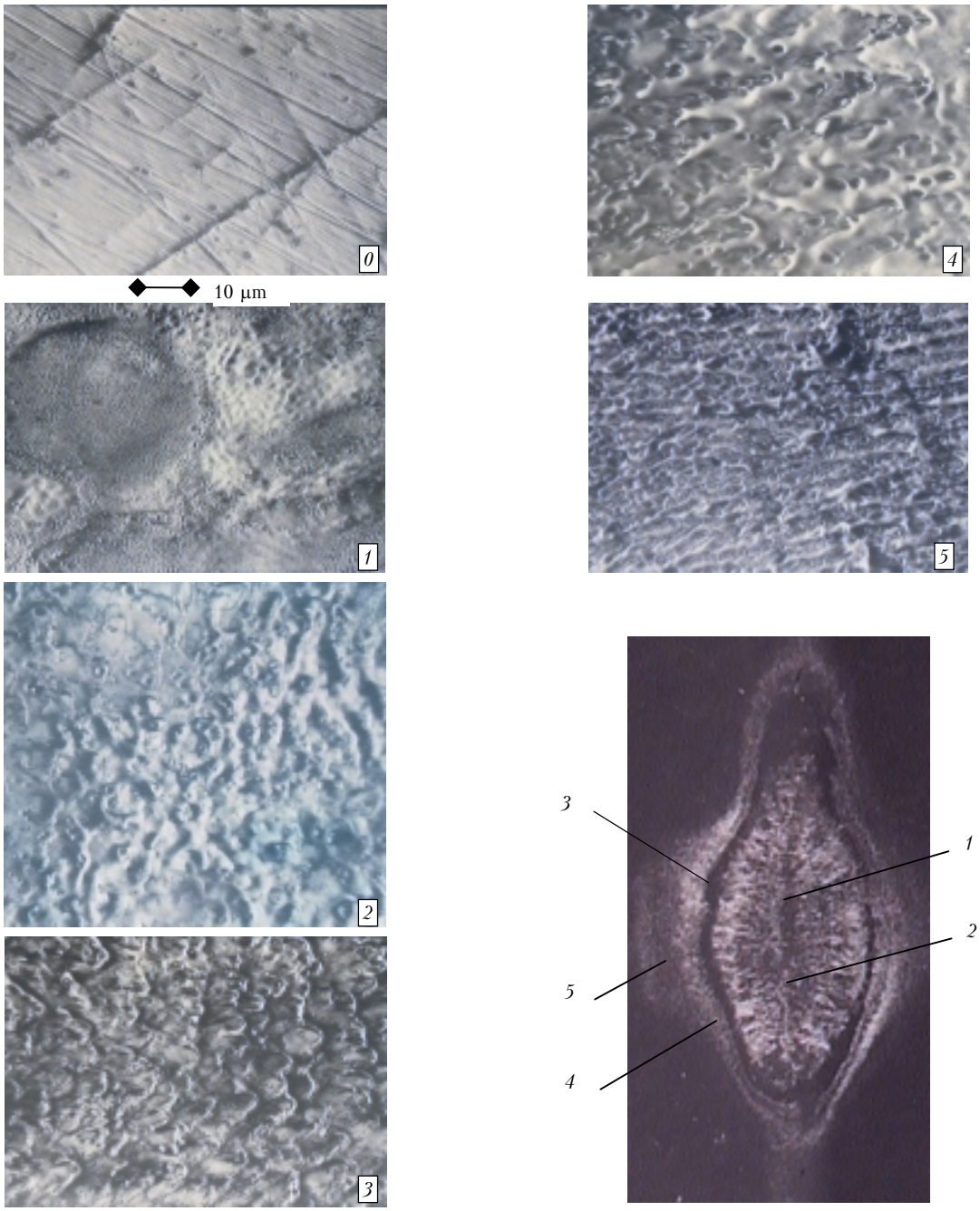

Fig. 3. The photograph of the print of the HF-laser radiation focused on the surface of carbon steel 4140 (at the bottom to the right) and microphotographs of separate parts of the spot on an enlarged scale (exposure No. 0 is a nonirradiated surface).

Figure 3 shows the photograph of the laser radiation print on the surface of stainless steel (at the bottom to the right) as well as microphotographs of individual areas (Nos. 0–5 in the figure) at large magnification of the microscope. It should be noted that these results on the action of laser radiation on the metal surface are preliminary. Further these experiments will be continued with coatings sprayed on metals.

Acknowledgment

This work was supported by ISTC, project No 1206.

References

1. A.S. Bugaev, N.N. Koval, V.F. Tarasenko, and A.V. Fedenev, Kvant. Elektron. **19**, No. 11, 1064–1067 (1992).

2. E.N. Abdullin, S.P. Bugaev, A.M. Efremov, V.B. Zorin, B.M. Kovalchuk, V.V. Kremnev, S.V. Loginov, G.A. Mesyats, V.S. Tolkachev, and P.M. Shchanin, Prib. Tekh. Eksp., No. 5, 138–141 (1993).

3. E.N. Abdullin, S.I. Gorbachev, A.I. Efremov, B.M. Kovalchuk, S.V. Loginov, V.S. Skakun, V.F. Tarasenko,

V.S. Tolkachev, A.V. Fedenev, E.A. Fomin, and P.M. Shchanin, Kvant. Elektron. **20**, No. 7, 652–656 (1993).
4. B.M. Kovalchuk, V.F. Tarasenko, A.V. Fedenev, Atmos. Oceanic Opt. **9**, No. 2, 98–99 (1996).
5. V.F. Tarasenko, A.N. Panchenko, and E.H. Baksht, in: *Proc. of the Int. Cong. LASERS 2000,* ed. by V.J. Corcoran and T.A. Corcoran (STS Press, McLean, VA, 2001), pp. 330–333.
6. E.N. Abdullin, A.M. Efremov, B.M. Koval'chuk, V.M. Orlovskii, A.N. Panchenko, V.V. Ryzhev, E.A. Sosnin, V.F. Tarasenko, and I.Yu. Turchanovskii, Kvant. Elektron. **24**, No. 9, 781–785 (1997).
7. E.N. Abdullin, A.M. Efremov, B.M. Kovalchuk, V.M. Orlovskii, A.N. Panchenko, E.A. Sosnin, V.F. Tarasenko, and A.V. Fedenev, Pis'ma Zh. Tekh. Fiz. **23**, No. 5, 58–64 (1997).
8. V.F. Tarasenko, E.H. Baksht, A.V. Fedenev, V.M. Orlovskii, A.N. Panchenko, V.S. Skakun, and E.A. Sosnin, Proc. SPIE **3343**, 715–724 (1998).
9. V.F. Tarasenko, S.V. Alekseev, M.V. Erofeev, and V.M. Orlovskii, in: *Proc. of the Int. Conf. LASERS 2000,* ed. by V.J. Corcoran and T.A. Corcoran (STS Press, McLean, VA, 2001), pp. 317–323.
10. J. Shein, K.M. Campbell, R.R. Prasad, E.I. Lipatov, A.N. Panchenko, V.F. Tarasenko, and M. Krisman, in: *Proc. of the Int. Conf. LASERS 2000,* ed. by V.J. Corcoran and T.A. Corcoran (STS Press, MclLean, VA, 2001), pp. 229–234.
11. V.F. Tarasenko, E.H. Baksht, S.E. Kunts, A.V. Fedenev, A.N. Panchenko, A.A. Kim, A.A. Sinebrjukhov, and S.V. Volkov, Proc. SPIE **4276**, 99–104 (2001).